Space Vector-Based Analytical Analysis of the Input Current Distortion of a Three-Phase Discontinuous-Mode Boost Rectifier System

Johann W. Kolar, *Member, IEEE*, Hans Ertl, *Member, IEEE*, and Franz C. Zach, *Member, IEEE*

***Abstract*—In this paper the low frequency harmonic distortion of the mains current of a three-phase single-switch discontinuous-mode boost-rectifier is calculated. The system analysis is based on application of space vector calculus and on substitution of discontinuous time shapes within a pulse period by quasicontinuous time shapes. The quasicontinuous time shapes are defined by averaging over the pulse period. The dependency of the shape of the input currents on the voltage transformation ratio is given for various control methods in analytical form. The results of the theoretical analysis are verified by digital simulation and by measurements on a laboratory model. A good consistency of the results has been found.**

NOMENCLATURE

C	output capacitor
C_N	mains filter capacitor
D	output diode
D_k	diodes of the three-phase rectifier bridge ($k = 1 \ldots 6$)
f_N, f_P	mains frequency, pulse frequency
i_D	output diode current
$i_{N,(RST)}$	mains phase currents
$\hat{I}_{D,(6i)}$	amplitude of the harmonic with order $6\,i$ ($i = 1, 2, 3 \ldots$) of the output diode current
i_T	transistor current
i_U	magnitude of the space vector $\underline{i}_U$
$\underline{i}_U$	space vector assigned to $i_{U,(RST)}$
$i_{U,(RST)}$	input currents of the three-phase rectifier bridge
$I_{N,(k)}$	Fourier coefficient of the mains phase current ($k = 5, 7, 11, 13 \ldots$)
$\hat{I}_{N,(k)}$	amplitude of the mains current harmonic with order k
I_O	load (output) current
k_P	gain of the output voltage controller
L_N	mains filter inductances
L_U	AC side series inductances
M	voltage transformation ratio
p_O	output power
$R(s)$	transfer function of the output voltage controller
R_O	load resistance
R_N	power-equivalent input resistance of the converter (regarding the fundamental); star connection
t	(global) time
t_μ	local time (within a pulse period)
$t_{\mu,1}$	turn-on time of power transistor T
T	power transistor
T_N	mains fundamental period
T_P	pulse period
$\underline{u}_N$	space vector assigned to the $u_{N,(RST)}$
$u_{N,(RST)}$	mains phase voltages
u_O	DC output voltage
u_T	transistor voltage
u_U	magnitude of $\underline{u}_U$
$\underline{u}_U$	space vector assigned to $u_{U,(RST)}$
$u_{U,(RST)}$	input phase voltages of the three-phase rectifier bridge
$\hat{U}_N$	amplitude of mains phase voltage (fundamental), magnitude of space vector $\underline{u}_N$
δ'_P	turn-on time $t_{\mu,1}$ of T related to the local conduction interval of three-phase rectifier bridge
δ_P	rated turn-on interval of T
φ_N	phase assigned to time t ($\varphi_N = \omega_N t$)
ω_N	mains angular frequency

lower case letters: characterizing (local or global) time-dependent quantities

upper case letters: characterizing time-independent global mean or rms values

Indices:

avg	linear mean value
n	reference value (basis) of the normalization
r	normalized (rated) quantity
rms	quadratic mean value (rms value)
$t_{\mu,i}$	time assignment of a local current value
(RST)	phase R or phase S or phase T, respectively
α, β	components of a space vector
μ	local time within a pulse period

Manuscript received March 17, 1993; revised May 13, 1995.

The authors are with the Technical University Vienna, Power Electronics Section, A-1040 Vienna, Austria.

IEEE Log Number 9414912.

I. INTRODUCTION

TODAY in most cases uncontrolled three-phase bridge circuits are used for coupling of converter systems with voltage dc link to the three-phase mains. Such converters of usually low and medium power are used widely in the industrial automation and process technology.

Regarding the mains behavior this concept is characterized by the presence of high low-frequency mains current harmonics especially for direct mains connection (without smoothing inductances on ac or dc side) or discontinuous conduction

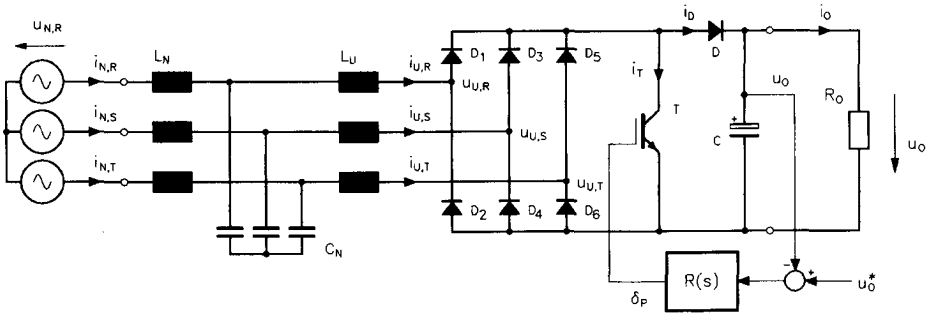

Fig. 1. Structure of the power circuit of a three-phase discontinuous-mode boost rectifier. Filtering of the high-frequency spectral components of the discontinuous input currents $i_{U,(RST)}$ of the three-phase diode bridge by mains filter L_N, C_N. The supplying mains is replaced by a star-connection of ideal voltage sources $u_{N,(RST)}$. The relative on-time δ_P of the power transistor T shall be given by a controller $R(s)$ in dependency on the output voltage control error.

of the diode bridge, respectively. Besides higher transmission losses these currents result in a distortion of the mains voltage due to the inner impedance of the supplying mains. This voltage distortion at the point of common coupling may cause an influence or malfunction of other systems. A further basic disadvantage of uncontrolled rectification is that the output voltage is in direct dependency on the voltage of the supplying mains. The mains voltage tolerance band therefore has to be considered for the dimensioning of the load side converter by increasing the VA-rating. Furthermore, a system operation for very much different nominal mains voltages is only possible by using a matching transformer which results in increased system weight and size.

In [1] a three-phase pulse rectifier system (a three-phase discontinuous-mode boost rectifier, cf. Fig. 1) is introduced which shows a remarkably simple structure of the power and control circuits. As compared to uncontrolled rectification with line commutation, this system also has the advantage of controllable output voltage besides low distortion of the input current. Furthermore, it results in an approximately resistive mains load behavior. However, the system analysis given in [1] using a single-phase equivalent circuit is limited to high values of the output voltage (related to the mains voltage). This means that the converter operation is not treated by this method in the case of the especially interesting region of an output voltage U_O = 620 V . . . 820 V. This output voltage is a possible dc link voltage level, e.g., for PWM inverter systems for operation from the European low-voltage mains with 380 V_{rms} line-to-line voltage.

The analysis of the low-frequency mains current harmonics for the circuit given in [1] is the topic of this paper. The calculation of the power factor is omitted due to the relative low significance regarding the influence on the mains. The importance especially of the low-frequency current harmonics for the judgement of the influence on the mains is due to the high low-frequency harmonic content of the public mains whose limitation based on recommendations (IEEE 519) and regulations (IEC 555-2) is strived for.

The analysis of the system behavior is performed based on the space vector calculus which allows a direct and clear mathematical description of three-phase systems. This avoids the use of a single-phase equivalent circuit as used in [1] which shows only a limited validity. The mains currents remaining after filtering out the high-frequency harmonics of the discontinuous input currents of the rectifier are calculated in analytically closed form. There, a local averaging is used which is related to one pulse period. For pulse frequencies being sufficiently higher than the mains frequency, this approximation shows high accuracy. The time shape and the low-order mains current harmonics are shown graphically for different control methods in dependency on the converter voltage transfer ratio. Finally, the results of the theoretical analysis are verified by digital simulation and by measurements on a laboratory model. A good consistency of the results is obtained.

II. Principle of Operation

As already mentioned, the system of Fig. 1 shows the structure of a three-phase single-switch discontinuous-mode boost converter. It can be regarded as being built up based on a three-phase extension of a boost converter [2] as applied for power factor correction of single-phase unidirectional ac-dc power conversion. For low dynamics and constant pulse frequency f_P the control of the converter is performed with an on-time $t_{\mu,1}$ of the power transistor T being approximately constant over the fundamental period. A synchronization of f_P and mains frequency f_N is not necessary for $f_P \gg f_N$. The output voltage has a lower limit according to the boost converter structure as given by the amplitude of the mains line-to-line voltage $\sqrt{3}\hat{U}_N$.

For illustrating the principle of operation in Fig. 2, the conduction states of the converter are shown within a pulse period $t_\mu \in [0, T_P]$. Regarding the values of the mains phase voltages we assume $u_{N,R} > 0$, $u_{N,T} \leq u_{N,S} \leq 0$ as being valid for an interval $\pi/6$ of the mains (fundamental) period. The mains phase voltages $u_{N,(RST)}$ are considered approximately constant within a pulse period. Due to the low-pass characteristic of the mains filter L_N, C_N, the mains voltage can be thought to be present directly on the filter output. Before transistor T is turned on we have $i_{U,R} = i_{U,S} = i_{U,T} = 0$ according to the discontinuous conduction mode. The dc output voltage u_O is assumed to be sufficiently higher than the peak value of the line-to-line mains voltage. Therefore, we have the output diode D and the diodes $D_1 \ldots D_6$ of the three-phase bridge rectifier in blocking state.

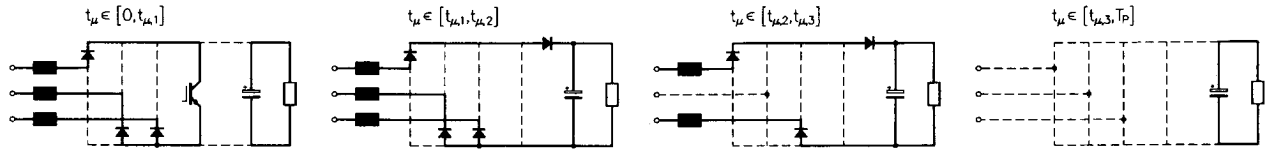

Fig. 2. Sequence of the conduction states of a three-phase single-switch discontinuous-mode boost rectifier within a pulse period $t_\mu \in [0, T_P]$ for $u_{N,R} > 0$, $u_{N,T} \leq u_{N,S} \leq 0$. t_μ denotes a local time running within the pulse period. The position of the considered pulse interval within the fundamental period is determined by the global time t or by the phase angle $\varphi_N = \omega_N t$ (ω_N = angular speed of the mains), respectively.

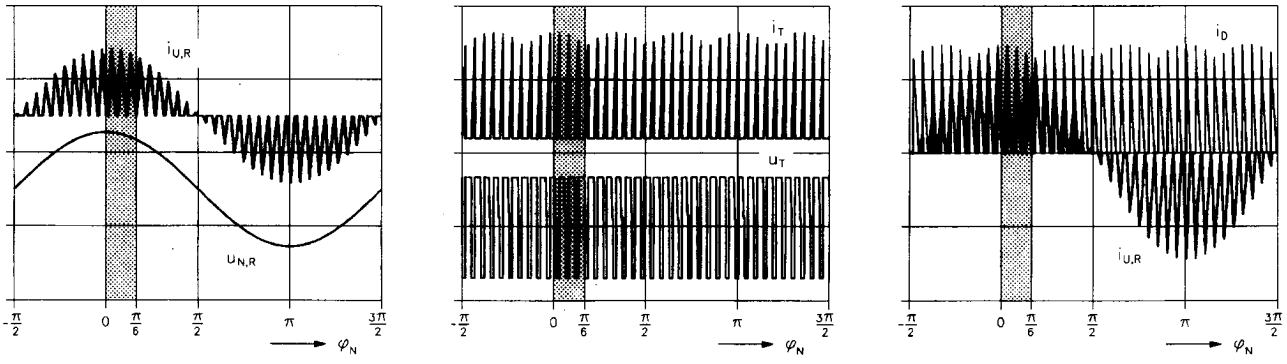

Fig. 3. Digital simulation of a three-phase discontinuous-mode boost rectifier without mains filter L_N, C_N, operated with constant switching frequency f_P. Turn-on interval $t_\mu \in [0, t_{\mu,1}]$ constant over the fundamental period; representation for one fundamental period $\varphi_N \in [-\frac{\pi}{2}, \frac{3\pi}{2}]$; dotted area: angle interval $\varphi_N \in [0, \frac{\pi}{6}]$ considered for the analysis of the system behavior; (a) input phase current $i_{U,R}$ (40 A/div) and related mains voltage $u_{N,R}$ (400 V/div); (b) current i_T through transistor T (25 A/div) and voltage u_T across T (600 V/div); (c) current i_D through output diode D and current $i_{U,R}$ (both 25 A/div); parameters: $U_{N,\mathrm{rms}} = 220$ V, $U_O = 820$ V, $f_N = 50$ Hz, $f_P = 1/T_P = 1.95$ kHz, $L_U = 1.5$ mH, $P_O = 7.5$ kW.

T shall be turned on at $t_\mu = 0$. The rate of rise of the phase currents due to the short circuit of the diode bridge on the dc side is defined by the driving mains phase voltages and by the inductances L_U. The turn-off of T in $t_{\mu,1}$ (as given by the control circuit) is followed by demagnetization of the inductances L_U via diode D into the capacitor C buffering the output voltage. There, only within the first demagnetization interval $t_\mu \in [t_{\mu,1}, t_{\mu,2}]$ all phases conduct current. In $t_{\mu,2}$ that phase current which shows the smallest absolute value at $t_{\mu,1}$ becomes 0 (in our case, $i_{U,S}$). The following second demagnetization interval (demagnetization of the remaining phases R and T which now conduct equal currents with opposite signs) is finished at $t_{\mu,3}$. There, one has to guarantee $t_{\mu,3} \leq T_P$ for discontinuous mode by appropriate dimensioning of L_U. Therefore, the system can be analyzed only by a rough approximation using a single-phase equivalent circuit because this basically does not include the second demagnetization interval.

Fig. 3 shows the shape of input current $i_{U,R}$ and mains phase voltage $u_{N,R}$ of the rectifier gained by digital simulation. For demonstration purposes the system is pulsed with low switching frequency. The discontinuous input phase currents $i_{U,(RST)}$ follow envelopes which are proportional to the respective phase voltages $u_{N,(RST)}$. By filtering out the spectral components having switching frequency by a mains filter L_N, C_N connected in series (cf. Fig. 1) we therefore obtain an approximately ohmic mains loading (referred to the fundamentals of the mains currents $i_{N,(RST)}$). One has to point out that due to the on-time of T being constant over the fundamental period the current guidance results directly from the mains voltage and not from a sinusoidal variation of the duty cycle of T.

Prior to the calculation of the low-frequency harmonics of the mains currents (cf. Section V) remaining after filtering we want to compile the assumptions made there, the definitions and the basics of the calculation method in the following.

III. Analysis Method

A. Assumptions

The analysis of the system is based on the following simplifying assumptions [3]:

- purely sinusoidal, symmetric mains voltage system $u_{N,(RST)}$
- the ripple of the voltages across the filtering capacitors C_N is negligible ($< 5\%$)
- the amplitudes of the fundamental voltage drops across the filtering inductances L_N are negligible as compared to the amplitude of the mains phase voltages $\hat{U}_N$; the voltages across C_N therefore are assumed to be impressed and equal to the mains phase voltages $u_{N,(RST)}$
- constant output voltage $u_O = U_O$ (ripple $< 5\%$)
- constant output current $i_O = I_O$
- $f_P > 200\, f_N$ or $T_P \ll T_N$, respectively (mains voltages approximately constant within a pulse period)
- ideal system components, especially neglection of losses, switching times etc.

It is of special importance to assume a sufficiently high switching frequency of the converter ($f_P \gg f_N$). As described in the following, this assumption allows a direct analytical calculation of the shape of the filtered converter input current.

According to the phase-symmetric structure of the power electronic system and to the assumed symmetry of the mains

voltage we can limit the description of the system behavior as given in Section IV to the interval $\varphi_N \in [0, \frac{\pi}{6}]$ (cf. Fig. 3). By simple symmetry considerations this interval can be extended to the entire fundamental period (cf. section III-B, (2)).

B. Quasi-Continuous Approximation

For a practical realization of the system one should strive for $f_P > 20$ kHz, i.e., above the audible spectrum. A further increase of f_P results in a reduced filtering effort. This seems to be realizable also for higher output power P_O because the discontinuous mode avoids a stress of T due to the reverse recovery current of D.

Based on the assumption of a high f_P a quasicontinuous analytical approximation

$$i_{N,(RST)}(\varphi_N) = i_{U,(RST),\text{avg}} = \frac{1}{T_P}\int_0^{T_P} i_{U,(RST)}(t_\mu)\, dt_\mu \tag{1}$$

of the mains currents can be calculated [4]–[6]. This is achieved by using an averaging of the discontinuous currents $i_{U,(RST)}$. The averaging suppresses local variations with switching frequency. There, t_μ denotes a local time running within the pulse period, φ_N gives the position of the pulse interval within the fundamental period.

Due to the assumed symmetry of the mains voltage system the shape of, e.g., $i_{N,R}$ within $\varphi_N \in [\frac{\pi}{6}, \frac{\pi}{2}]$ can be given directly by

$$i_{N,R} = \begin{cases} -i_{U,T,\text{avg}}(\frac{\pi}{3} - \varphi_N) & \varphi_N \in [\frac{\pi}{6}, \frac{\pi}{3}] \\ -i_{U,S,\text{avg}}(\varphi_N - \frac{\pi}{3}) & \varphi_N \in [\frac{\pi}{3}, \frac{\pi}{2}] \end{cases} \tag{2}$$

via an appropriate shift of the shapes of the phase currents $i_{N,S}$ and $i_{N,T}$ which have been calculated for the analyzed interval $\varphi_N \in [0, \frac{\pi}{6}]$.

As a check by digital simulation (cf. Section VI) shows, for $f_P \geq 500\, f_N$ the deviation remains below 1% as compared to the exact values of the low-frequency harmonics of $i_{N,(RST)}$.

Besides the shape of the mains current, also the mean value of the output diode current which defines the output power of the system according to

$$P_O = U_O\, I_{D,\text{avg}} \tag{3}$$

can be given in analytically closed form

$$I_{D,\text{avg}} = \frac{6}{\pi}\int_0^{\frac{\pi}{6}} i_{D,\text{avg}}(\varphi_N)\, d\varphi_N \tag{4}$$

(also shown in Section V). Analogous to (1) we have for the local mean value of the diode current for the considered angle interval $\varphi_N \in [0, \frac{\pi}{6}]$ (cf. Fig. 5):

$$i_{D,\text{avg}} = \frac{1}{T_P}\int_{t_{\mu,1}}^{T_P} i_R(t_\mu)\, dt_\mu. \tag{5}$$

C. Space Vectors

The space vector calculus [7] is used for special clearness and due to a simpler calculation (compared to the methods using phase quantities).

For the definition of the complex phasor associated with a triple of phase quantities we have (for the example of the converter input currents)

$$\underline{i}_U = (i_{U,\alpha} + j\, i_{U,\beta}) = \frac{2}{3}(i_{U,R} + \underline{a} i_{U,S} + \underline{a}^2 i_{U,T}) \tag{6}$$
$$\underline{a} = (-\frac{1}{2} + j\frac{\sqrt{3}}{2}).$$

Remark: Space vectors are used for the description of space distributions of electrical and magnetic quantities in the area of three-phase ac machines. Here, however, formally equal defined complex phasors describe the *time-behavior* of the phase quantities. One should call the complex quantity $\underline{i}_U$ defined by (6) therefore correctly a *three-phase phasor* of the instantaneous values of the input currents $i_{U,(RST)}$ of the diode bridge. Because the literature of power electronics does not make a difference between these two aspects, we also will use the term "space vector" in the following.

For the back-transformation of the space vector components $i_{U,\alpha}$ and $i_{U,\beta}$ into phase quantities there follows

$$\begin{aligned} i_{U,R} &= i_{U,\alpha} \\ i_{U,S} &= -\frac{1}{2} i_{U,\alpha} + \frac{\sqrt{3}}{2} i_{U,\beta} \\ i_{U,T} &= -\frac{1}{2} i_{U,\alpha} - \frac{\sqrt{3}}{2} i_{U,\beta}. \end{aligned} \tag{7}$$

D. Normalization

For a wide applicability and a simple transfer of the relationships derived here, we want to agree on the following normalizations

$$\begin{aligned} t_{\mu,i,r} &= \frac{1}{T_P}\, t_{\mu,i} \\ u_{i,r} &= \frac{1}{U_O}\, u_i \\ i_{i,r} &= \frac{1}{I_n}\, i_i \\ p_{i,r} &= \frac{1}{P_n}\, p_i. \end{aligned} \tag{8}$$

Into the basis quantities

$$I_n = \frac{2}{3} U_O \frac{T_P}{L_U} \qquad P_n = \frac{2}{3} U_O^2 \frac{T_P}{L_U} \tag{9}$$

we include the parameters which directly influence the system behavior. If one includes the output voltage (being controlled to a fixed value) instead of, e.g., the mains phase voltage amplitude into the normalization basis of currents and powers one can avoid a change of the basis quantities for changing mains voltage conditions (due to the input voltage tolerance band or different nominal values of $\hat{U}_N$).

With (3), (8), and (9) we have for the rated system output power

$$P_{O,r} \equiv I_{D,\text{avg},r}. \tag{10}$$

E. Definitions

In the following the definitions of important characteristic system quantities are summarized briefly. For the characterization of the system voltage transfer ratio the ratio of output voltage to the amplitude of the mains line-to-line voltage is used according to

$$M = \frac{U_O}{\sqrt{3}\hat{U}_N} \qquad M \geq 1\ . \tag{11}$$

For the relative on-time of the transistor T we define

$$\delta_P = \frac{t_{\mu,1}}{T_P}. \tag{12}$$

Because the shape of the envelope of the discontinuous input phase current $i_{U,i}$ is proportional to the related phase voltage (cf. Fig. 3(a)) no phase shift of the fundamental of the input phase current and of the related phase voltage occurs at the mains filter output. As noted in Section III-A, now the filter damping at mains frequency can be neglected due to the fact that the cut-off frequency lies substantially above the mains frequency for practically realized systems. Accordingly, the filter output voltage can be set approximately equal to the mains voltage or assumed being purely sinusoidal. Therefore, the power consumption of the rectifier system corresponds to a star-connection of equivalent resistors R_N lying at the output of the mains filter [8], [9]. Based on the power balance between the ac and the dc side of the system

$$P_O = U_O I_{D,\mathrm{avg}} = \frac{3}{2}\hat{U}_N \hat{I}_{U,(1)} = \frac{3}{2}\frac{\hat{U}_N^2}{R_N} \tag{13}$$

there follows under consideration of (11) and of the relations given in Section III-D

$$R_N = \frac{3}{4}\frac{L}{T_P} M^{-2} I_{D,\mathrm{avg},r}^{-1}. \tag{14}$$

The real power contributions formed as product of equal order harmonics of the rectifier input current and of the filter output voltage are not covered by R_N. R_N represents an equivalent quantity being related to the fundamentals. The parameter dependency of R_N yields a clear conclusion about the controllability of the main power flow of the system.

Remark: It is important to note that R_N describes only the main power flow but not the rectifier input characteristic which defines the instantaneous current consumption. A corresponding equivalent resistance (the system input impedance) is to be defined by the ratio of the mains voltage and the rectifier input current space vectors $\underline{r}_U = \underline{u}_N/\underline{i}_U$. It shows a time-dependent complex value. The occurrence of low-frequency input current harmonics (cf. Fig. 7) which cannot be explained by a time-constant resistive load R_N becomes clear, therefore.

The fundamental $i_{N,(1)}$ of the mains current is formed by the sum of the resistive input current $i_{U,(1)}$ of the system and by the current consumption of the mains filter being capacitive at mains frequency. Therefore, especially for low output power mains current and mains voltage fundamental will not be in phase; resistive behavior of the rectifier system is given only regarding the fundamental of the mains filter output voltage, but not with respect to the mains voltage. For the sake of concentrating on the essentials we want to neglect the capacitive current contribution at the fundamental frequency as caused by the mains filter; only the resistive contribution of the mains current shall be considered, or $\hat{I}_{N,(1)} = \hat{I}_{U,(1)}$ shall be set in the following.

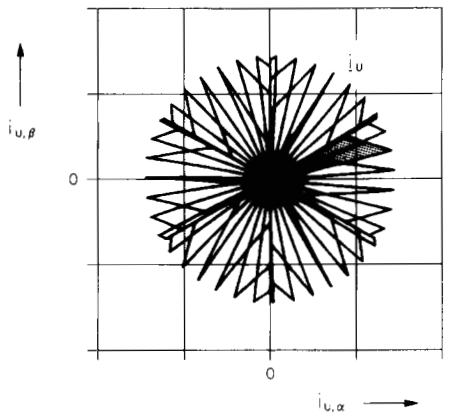

Fig. 4. Trajectory of $\underline{i}_U$ related to Fig. 3 (25 A/div); representation for one fundamental period; within each pulse period the trajectory describes an acute-angled triangle (marked by the dotted area).

IV. Basic System Equations

According to (1), the calculation of the local mean values $i_{N,(RST)}$ defining the shape of the mains phase currents is related to the shape of the discontinuous input currents $i_{U,(RST)}(t_\mu)$ of the bridge rectifier. Its analysis is the topic of this section.

As can be seen from Fig. 4, the trajectory of $\underline{i}_U$ describes an acute-angled triangle within each pulse period. The mathematical description of these trajectory segments which completely describe the shape of the phase currents within the pulse period according to Section III-A can be limited to $\varphi_N \in [0, \frac{\pi}{6}]$ (cf. Fig. 5). The assumed symmetric and purely sinusoidal system of mains voltages

$$\begin{aligned} u_{N,R} &= \hat{U}_N \cos(\varphi_N) \\ u_{N,S} &= \hat{U}_N \cos(\varphi_N - \frac{2\pi}{3}) \\ u_{N,T} &= \hat{U}_N \cos(\varphi_N + \frac{2\pi}{3}) \end{aligned} \tag{15}$$

is described by the mains voltage space vector (rotating with constant angular speed ω_N)

$$\underline{u}_N = \hat{U}_N \exp(j\varphi_N) \qquad \varphi_N = \omega_N t. \tag{16}$$

$\underline{u}_N$ is approximated by a phasor being fixed within the considered pulse period. Due to the discontinuous operation we have $\underline{i}_U = 0$ before T is turned on in $t_\mu = 0$. The linear rate of rise of the phase currents within $t_\mu \in [0, t_{\mu,1}]$ (cf. Fig. 5, right hand side) corresponds to a linear rise of the magnitude of the space vector $\underline{i}_U$ in the direction of $\underline{u}_N$. After turning off T at $t_{\mu,1}$ the voltage space vector defining the current change is given by $\underline{u}_N - \underline{u}_{U,[100]}$ ($\underline{u}_{U,[100]}$: space vector of converter input voltages when diodes D_1, D_4 and D_6 are conducting). When $\underline{i}_U$ reaches the limit $i_{U,S} = 0$ at $t_{\mu,2}$ (i.e., when the phase current showing the smallest absolute value at $t_{\mu,1}$ becomes

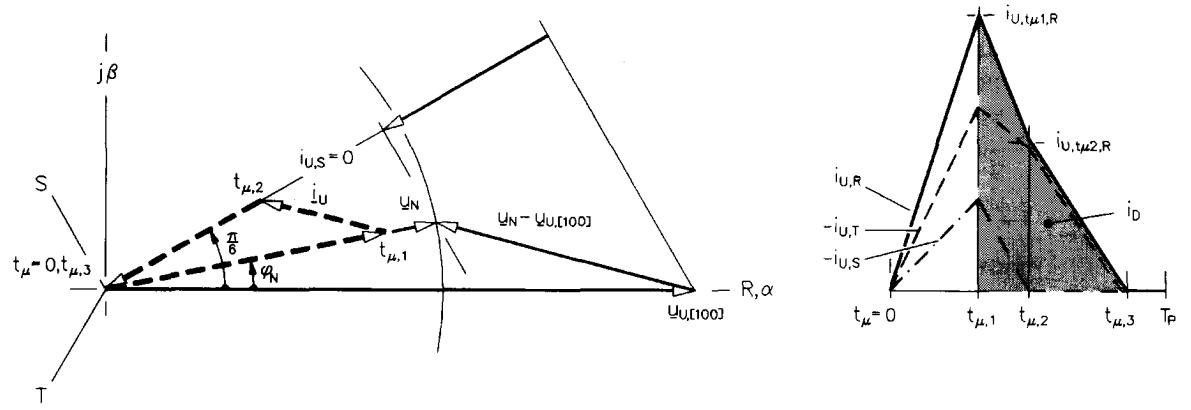

Fig. 5. Description of the operating behavior by space vector calculus: trajectory of $\underline{i}_U$ and related time shape of the converter input currents $i_{U,(RST)}$ and of output diode current i_D (marked by the dotted area) within one pulse period $t_\mu \in [0, T_P]$ for $u_{N,R} > 0$, $u_{N,T} \leq u_{N,S} \leq 0$ (cf. Fig. 2); $\underline{u}_N$: space vector of the mains phase voltages; $\underline{u}_{U,[100]}$: space vector of the input voltages of the three-phase diode bridge when diodes D_1, D_4 and D_6 are conducting (cf. Fig. 1); phase $\varphi_N = \omega_N t$ defines the time position of the pulse interval considered within the fundamental period $\varphi_N \in [-\frac{\pi}{2}, \frac{3\pi}{2}]$; parameter: $M = 1.5$.

0), the second demagnetization interval begins. From now on the current-driving voltage is given only by the projection of $\underline{u}_N - \underline{u}_{U,[100]}$ onto the axis $i_{U,S} = 0$. The demagnetization of the inductances L_U is finished at $t_{\mu,3}$. For discontinuous operation one has to guarantee $t_{\mu,3} \leq T_P$ therefore.

Remark: The considerations made show clearly the only limited validity of a system analysis based on a single-phase equivalent circuit. There, a second demagnetization phase is basically not included. Therefore, especially for small values of M (≤ 2) considerable errors in modeling result.

Considering the differential equation

$$L_U \frac{d\underline{i}_U}{dt_\mu} = \underline{u}_N - \underline{u}_U(\underline{i}_U, t_\mu) \tag{17}$$

of the ac side system part there follows for the space vector components and time intervals ($\Delta t_{\mu,ji} = t_{\mu,j} - t_{\mu,i}$) defining the trajectory of $\underline{i}_U$ (consisting of approximately straight line segments),

$$\begin{aligned} &t_\mu = t_{\mu,1}: \\ &i_{U,t\mu1,\alpha,r} = \frac{\sqrt{3}}{2}\,\delta_P\, M^{-1}\cos(\varphi_N) \\ &i_{U,t\mu1,\beta,r} = \frac{\sqrt{3}}{2}\,\delta_P\, M^{-1}\sin(\varphi_N) \qquad (18) \\ &t_\mu = t_{\mu,2}: \\ &i_{U,t\mu2,\alpha,r} = \frac{3}{2}\,\delta_P\, M^{-1}\,\frac{\sin(\varphi_N)}{1+\sqrt{3}M^{-1}\sin(\varphi_N-\frac{\pi}{6})} \\ &i_{U,t\mu2,\beta,r} = \frac{\sqrt{3}}{2}\,\delta_P\, M^{-1}\,\frac{\sin(\varphi_N)}{1+\sqrt{3}M^{-1}\sin(\varphi_N-\frac{\pi}{6})} \qquad (19) \end{aligned}$$

and see (20), shown at the bottom of the page. The local current flow interval of the three-pase rectifier bridge related to the turn-on time of T results as

$$\delta_P'^{-1} = \frac{t_{\mu,3}}{t_{\mu,1}} = \frac{1}{1 - M^{-1}\cos(\varphi_N - \frac{\pi}{6})}. \tag{21}$$

Somewhat surprisingly there follows a relationship being valid in an analog manner for dc-dc boost converters. In the case at hand only the (constant) input voltage of the dc-dc converter related to the output voltage has to be replaced by the three-phase rectified mains voltage (for $\varphi_N \in [0, \frac{\pi}{6}]$: $u_{N,RT,r} = u_{N,R,r} - u_{N,T,r} = M^{-1}\cos(\varphi_N - \frac{\pi}{6})$; cf. also [10, (8)]).

V. Mains Current Harmonics

The analyses of the operation of three-phase single-switch discontinuous-mode pulse rectifiers given in the literature are limited to the same control method, i.e., the control with constant turn-on time $t_{\mu,1}$ and constant pulse frequency f_P [1], [9]–[11].

The aim of this section is to calculate the mains current quality in dependency on M for various control methods. As a basis we have the situation given for constant turn-on time $t_{\mu,1}$ of T and constant f_P. This control method, to be called **control method I** is given for practical system realization only at the limit of a cut-off frequency of the output voltage control lying substantially below 6 f_N (or in the case of an open-loop system control).

As a further control method (**control method II**) the operation of the converter is analyzed at the border of the discontinuous mode. Furthermore, again $t_{\mu,1}$ shall be constant over the fundamental period. Turning on of T in this case

$$\begin{aligned} \Delta t_{\mu,21,r} &= \sqrt{3}\,\delta_P M^{-1}\,\frac{\sin(\frac{\pi}{6}-\varphi_N)}{1+\sqrt{3}M^{-1}\sin(\varphi_N-\frac{\pi}{6})} \\ \Delta t_{\mu,32,r} &= 2\,\delta_P M^{-1}\,\frac{\sin(\varphi_N)}{(1+\sqrt{3}M^{-1}\sin(\varphi_N-\frac{\pi}{6}))(1-M^{-1}\cos(\varphi_N-\frac{\pi}{6}))} \end{aligned} \tag{20}$$

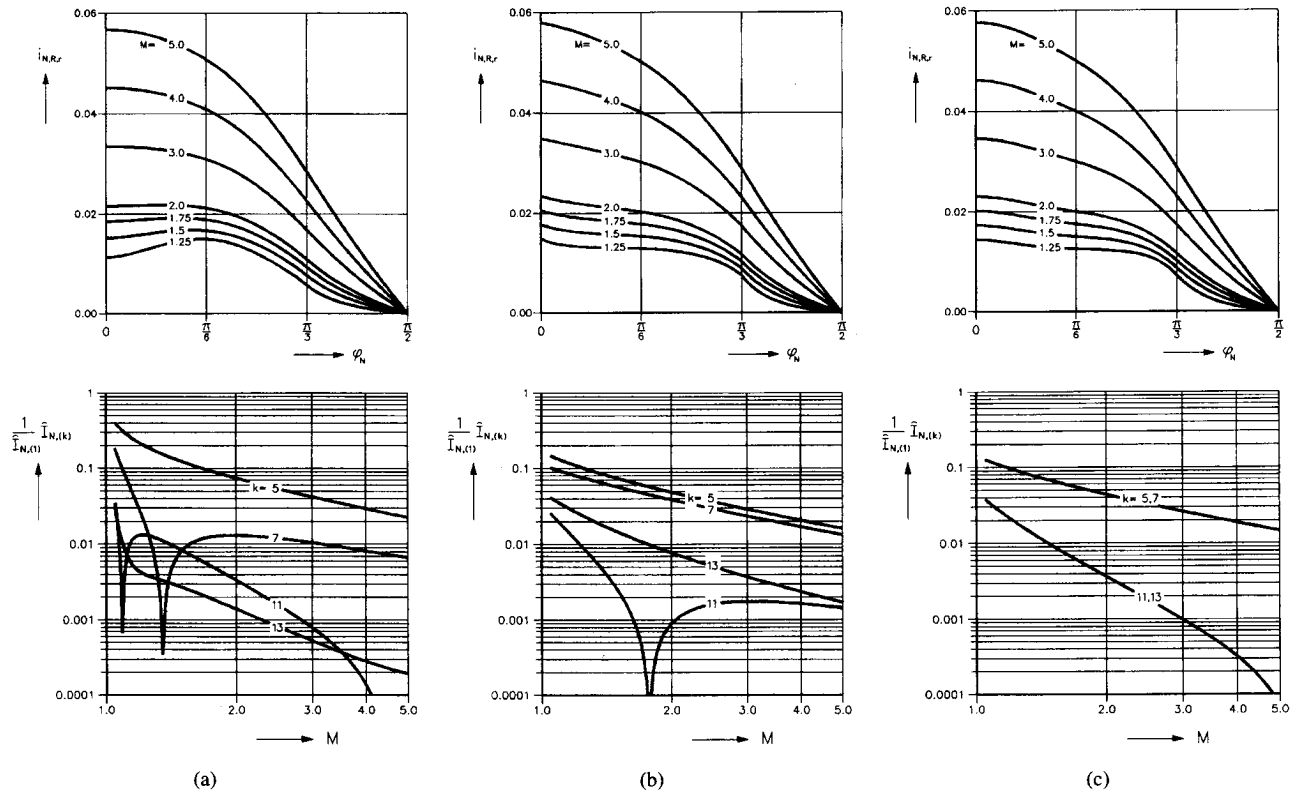

Fig. 6. Comparison of different control concepts. Representation of analytically calculated time behaviors (limited to a quarter fundamental period) and of the low frequency mains current harmonics $\hat{I}_{N,(k)}$ referred to the fundamental $\hat{I}_{N,(1)}$ in dependency on M for $P_{O,r} = 0.01$. (a) control method I: f_P and $t_{\mu,1}$ constant over the fundamental period; power pulsations on the dc side due to low frequency harmonics of $i_{N,(RST)}$ are not compensated; the cut-off frequency of the output voltage control loop lies substantially below $6f_N$. (b) control method II: As (a), but f_P not constant. T is turned on immediately after the end of the demagnetization of L_U at $t_{\mu,3}$; a current gap during $t_\mu \in [t_{\mu,3}, T_P]$ is avoided, the system is operated at the border to continuous mode. (c) control method III: As (a), but $t_{\mu,1}$ not constant. By highly dynamical output voltage control an approximately constant power flow on the dc side is impressed there (constant local mean value $i_{D,\text{avg}}$) by appropriate variation of $t_{\mu,1}$. The Fourier coefficients $I_{N,(k)}(k = (5,7);(11,13);\ldots)$ which lie in the vincinity of the multiples of 6 f_N show equal amplitude and opposite sign in this case; therefore, they do not occur as harmonics of $i_{D,\text{avg}}$ $(\hat{I}_{D,(6i)} \equiv 0, i = 1,2,\ldots)$.

takes place immediately after the end of the demagnetization interval at $t_{\mu,3}$. Due to the avoidance of a current gap $t_\mu \in [t_{\mu,3}, T_P]$ characterizing the discontinuous operation with constant f_P, maximum utilization of the power circuit components is achieved. The modulation of the pulse frequency with six times f_N (cf. Fig. 7) furthermore leads to a broader distribution of the high-frequency spectral components of $i_{U,(RST)}$. Due to the more even distribution of the same spectral power compared to constant f_P the filtering effort in order to satisfy the regulations for conducted electromagnetic influence (e.g., VDE 0871) is reduced especially for the region 10kHz $\leq f \leq$ 150kHz [12].

As mentioned, the operation of the system with constant $t_{\mu,1}$ is given only for the case of low dynamics (and if constant load current is assumed). This case is not very important for industrial applications. For high cut-off frequency of the control of u_O **(control method III)** the power oscillations with frequencies with $6i$ $(i = 1,2,3,\ldots)$ times f_N (which occur on the dc side for constant $t_{\mu,1}$ and constant f_P) are compensated via variation of $t_{\mu,1}$. This results ideally in a constant instantaneous local mean value $p_{O,\text{avg}}$ of the output power. If no buffering of load pulses, no buffering during voltage dips and no limitation of mains overvoltages is required, C (which usually would be an electrolytic capacitor) can be realized as a foil-type capacitor. This will have higher current carrying capability, may have much lower C and higher lifetime. This also increases the reliability of the converter [13].

Remark: As shown in [6, (57)], an increase of the output voltage control dynamics in single phase ac-dc converters leads to an increase of the low-frequency spectral components if the mains current as compared to the case with constant $t_{\mu,1}$. The reason is given by the pulsating instantaneous power of a single-phase system loaded with purely sinusoidal current. On the contrary, three-phase systems have a time-constant instantaneous value of power if the mains currents are purely sinusoidal and are in phase with the mains voltages. Therefore one can expect a *reduction* of the mains current harmonics for control method III. The distortion of $i_{N,(RST)}$ which remains to a reduced degree also for constant $p_{O,\text{avg}}$ is given by the instantaneous reactive input power [14] required for the system function. For the sake of brevity this shall not be treated here in detail.

In the following analytical approximations are given for the time behavior of $i_{N,(RST)}$ for the control methods described. The calculated current shapes are shown graphically in connection with the numerically gained low-frequency harmonics in dependency on M (cf. Fig. 6).

A. Control Method I

For the shape of the phase current $i_{N,R}$ we receive with (1), (2) and Section IV for constant $t_{\mu,1}$ and constant f_P (or constant δ_P)

$$\varphi_N \in [0, \frac{\pi}{6}]:$$
$$i_{N,R,r} = \frac{\sqrt{3}}{4}\delta_P^2 M^{-1} \frac{\cos(\varphi_N) - 2M^{-1}\cos(\varphi_N)\cos(\varphi_N + \frac{\pi}{6}) + \frac{\sqrt{3}}{2}M^{-1}}{\left(1 + \sqrt{3}M^{-1}\sin(\varphi_N - \frac{\pi}{6})\right)\left(1 - M^{-1}\cos(\varphi_N - \frac{\pi}{6})\right)} \quad (22)$$

$$\varphi_N \in [\frac{\pi}{6}, \frac{\pi}{3}]:$$
$$i_{N,R,r} = \frac{\sqrt{3}}{4}\delta_P^2 M^{-1} \frac{\cos(\varphi_N) + \frac{1}{2}M^{-1}\cos(2\varphi_N + \frac{\pi}{6})}{\left(1 - \sqrt{3}M^{-1}\sin(\varphi_N - \frac{\pi}{6})\right)\left(1 - M^{-1}\cos(\varphi_N - \frac{\pi}{6})\right)} \quad (23)$$

$$\varphi_N \in [\frac{\pi}{3}, \frac{\pi}{2}]:$$
$$i_{N,R,r} = \frac{\sqrt{3}}{4}\delta_P^2 M^{-1} \frac{\cos(\varphi_N)}{1 - \sqrt{3}M^{-1}\cos(\varphi_N)}. \quad (24)$$

The Fourier analysis of the mains current can be performed with the relations given in Section V-D.

The related local mean value $i_{D,\mathrm{avg},r}$ oscillating with 6 f_N (or the related local mean value of the output power $p_{O,\mathrm{avg},r} \equiv i_{D,\mathrm{avg},r}$) results in

$$i_{D,\mathrm{avg},r}(\varphi_N) = \frac{3}{8}\delta_P^2 M^{-2} \frac{1 - M^{-1}\cos(\varphi_N)\cos(2\varphi_N + \frac{\pi}{6})}{\left(1 + \sqrt{3}M^{-1}\sin(\varphi_N - \frac{\pi}{6})\right)\left(1 - M^{-1}\cos(\varphi_N - \frac{\pi}{6})\right)}. \quad (25)$$

With good approximation we have

$$i_{D,\mathrm{avg},r} \approx \frac{3}{8}\delta_P^2 \frac{M^{-2}}{1 - M^{-1}\cos(\varphi_N - \frac{\pi}{6})}. \quad (26)$$

Regarding the accuracy of this approximation we want to note that the maximum deviation with respect to (25) is determined essentially by the value of the voltage transformation ratio. As a simple calculation check shows, the relative error $f_{i_D,r}$ is limited to $f_{i_D,r} \leq +10\%$ for $M \geq 1.1$; for $M \geq 1.5$ we have $f_{i_D,r} \leq +5\%$ and for $M \geq 2.0$ $f_{i_D,r} \leq +3\%$. Basically, (26) gives an upper limit estimate.

The mean value of $i_{D,\mathrm{avg},r}$ related to the fundamental (or the related output power $P_{O,r} \equiv I_{D,\mathrm{avg},r}$) becomes (27) (see (27) at the bottom of this page). Approximately we can write

$$I_{D,\mathrm{avg},r} \approx \frac{9}{2\pi}\delta_P^2 \frac{M^{-1}}{\sqrt{M^2 - 1}} \tan^{-1}\frac{\sqrt{3}-1}{\sqrt{3}+1}\sqrt{\frac{M+1}{M-1}}. \quad (28)$$

This approximation being calculated based on (26) shows a relative error $f_{I_D,r} = +4.4\%$ for $M = 1.1$; for $M = 1.5$ we have $f_{I_D,r} = +2.4\%$ and for $M = 2.0$ $f_{I_D,r} = +1.6\%$. For larger values of the voltage transformation ratio a very good consistency of the estimate exists, therefore. With (28) there follows for the equivalent input resistance of the pulse rectifier system defined by (14)

$$R_N \approx \frac{\pi}{6}\frac{L_U}{T_P}\delta_P^{-2}\sqrt{1 - M^{-2}}\left(\tan^{-1}\frac{\sqrt{3}-1}{\sqrt{3}+1}\sqrt{\frac{M+1}{M-1}}\right)^{-1}. \quad (29)$$

R_N is dependent on M due to the duration of the demagnetization interval being dependent on the difference between input and output voltage (cf. (20)).

B. Control Method II

For the shape of the mains currents we have for turning on T again in $t_{\mu,3}$ (border of discontinuous mode) and for constant $t_{\mu,1}$

$$\varphi_N \in [0, \frac{\pi}{6}]:$$
$$i_{N,R,\mathrm{avg},r} = \frac{\sqrt{3}}{4}\delta_P M^{-1} \frac{\cos(\varphi_N) - M^{-1}\cos(2\varphi_N + \frac{\pi}{6})}{1 + \sqrt{3}M^{-1}\sin(\varphi_N - \frac{\pi}{6})} \quad (30)$$

$$\varphi_N \in [\frac{\pi}{6}, \frac{\pi}{3}]:$$
$$i_{N,R,\mathrm{avg},r} = \frac{\sqrt{3}}{4}\delta_P M^{-1} \frac{\cos(\varphi_N) + \frac{1}{2}M^{-1}\cos(2\varphi_N + \frac{\pi}{6})}{1 - \sqrt{3}M^{-1}\sin(\varphi_N - \frac{\pi}{6})} \quad (31)$$

$$\varphi_N \in [\frac{\pi}{3}, \frac{\pi}{2}]:$$
$$i_{N,R,\mathrm{avg},r} = \frac{\sqrt{3}}{4}\delta_P M^{-1} \frac{\cos(\varphi_N) - \frac{1}{2}M^{-1}\sin(2\varphi_N)}{1 - \sqrt{3}M^{-1}\cos(\varphi_N)}. \quad (32)$$

According to the system function the averaging of the converter input currents here has to be performed within the interval $t_\mu \in [0, t_{\mu,3}]$ and not within $T_P = \frac{1}{f_P}$. (As opposed to control methods I and III, there is no physical meaning of the frequency f_P which is included in the basis of the normalization, cf. (9).) For the defining equation of the local mean value we have therefore (by modifying (1))

$$i_{U,(RST),\mathrm{avg}}(\varphi_N) = \frac{1}{t_{\mu,3}}\int_0^{t_{\mu,3}} i_{U,(RST)}(t_\mu)\,dt_\mu. \quad (33)$$

$$I_{D,\mathrm{avg},r} = \frac{1}{2}\delta_P^2\left[\frac{3}{\pi}\left(\frac{M}{\sqrt{M^2-3}}\left(\tan^{-1}\frac{\sqrt{3}}{\sqrt{M^2-3}} + \tan^{-1}\frac{\frac{\sqrt{3}-1}{\sqrt{3}+1}M - \sqrt{3}}{\sqrt{M^2-3}}\right)\right.\right.$$
$$\left.\left. + \frac{3M}{\sqrt{M^2-1}}\tan^{-1}\frac{\sqrt{3}-1}{\sqrt{3}+1}\sqrt{\frac{M+1}{M-1}} - \frac{\sqrt{3}}{2}M^{-1}\right) - 1\right]. \quad (27)$$

Remark: For single-phase ac-dc boost converters being operated at the border to continuous mode we obtain a purely sinusoidal mains current for constant on-time of the power transistor [15]. In the case at hand there remains a gap $t_\mu \in [t_{\mu,2}, t_{\mu,3}]$ with $i_{U,S} = 0$ (in general, for that current which shows the lowest absolute value at $t_{\mu,1}$, cf. Fig. 5, right hand side). This is given despite of the fact that T is switched on again immediately at the end of the demagnetization (at $t_{\mu,3}$). This gap leads especially in the vincinity of the zero crossings of a mains phase current to a deviation from a sinusoidal shape (cf. Fig. 6). This deviation is characteristic for three-phase single-switch converters. Therefore, low-frequency harmonics occur contrary to the case of the corresponding single-phase system.

The local mean value of the related output power $p_{O,\mathrm{avg},r} \equiv i_{D,\mathrm{avg},r}$ is calculated as

$$i_{D,\mathrm{avg},r} = \frac{3}{8} M^{-2} \delta_P \frac{1 - M^{-1}\cos(\varphi_N)\cos(2\varphi_N + \frac{\pi}{6})}{1 + \sqrt{3}\, M^{-1} \sin(\varphi_N - \frac{\pi}{6})}. \tag{34}$$

A good approximation is given by

$$i_{D,\mathrm{avg},r} \approx \frac{3}{8} M^{-2} \delta_P . \tag{35}$$

Regarding the accuracy of this approximation the same is valid as has been said in conncetion with (26).

For the average value of $i_{D,\mathrm{avg},r}$ referred to the fundamental, or for the related output power $P_{O,r} \equiv I_{D,\mathrm{avg},r}$ we receive (36), shown at the bottom of the page. According to (35) one can give the approximation

$$I_{D,\mathrm{avg},r} \approx \frac{3}{8} M^{-2} \delta_P. \tag{37}$$

This approximation shows a relative error of $f_{I_D,r} \leq +4.0\%$ for $M \geq 1.1$; for $M \geq 1.5$ we have $f_{I_D,r} \leq +2.3\%$ and for $M \geq 2.0$ $f_{I_D,r} \leq +1.6\%$. With (37) we get for the equivalent input resistance

$$R_N \approx 2 \frac{L_U}{T_P} \delta_P^{-1}. \tag{38}$$

Accordingly, R_N is inverse proportional to the relative on-time of T. The output power P_O of the converter then is defined in a first approximation only by the input voltage and $t_{\mu,1}$ contrary to control method I (cf. (29)). R_N is not dependent on the actual value of U_O.

Remark: Equation (38) is valid in an analogous manner for the correspondingly controlled dc-dc boost converter where M has to be defined by the ratio of output and input dc voltages.

C. Control Method III

For highly dynamical control of the output voltage or for time-constant local mean value $p_{O,\mathrm{avg},r} = P_{O,r}$ or for constant

$$i_{D,\mathrm{avg},r} = P_{O,r} \tag{39}$$

and for constant f_P there follows via (25) for the relative turn-on time of T

$$\delta_P^2 = \frac{8}{3} M^2 P_{O,r} \frac{\left(1 + \sqrt{3} M^{-1} \sin(\varphi_N - \frac{\pi}{6})\right)\left(1 - M^{-1}\cos(\varphi_N - \frac{\pi}{6})\right)}{1 - M^{-1}\cos(\varphi_N)\cos(2\varphi_N + \frac{\pi}{6})}. \tag{40}$$

(δ_P has to be supplied by the controller $R(s)$, cf. Fig. 1). A good approximation is given by

$$\delta_P^2 \approx \frac{8}{3} M^2 P_{O,r} \left(1 - M^{-1}\cos(\varphi_N - \frac{\pi}{6})\right). \tag{41}$$

As (26) and (35) also this approximation is obtained by the estimation $(1 - M^{-1}\cos(\varphi_N)\cos(2\varphi_N + \frac{\pi}{6}))(1 + \sqrt{3}M^{-1}\sin(\varphi_N - \frac{\pi}{6}))^{-1} \approx 1$. For the accuracy the same is valid as has been said in connction with (26).

The shape of the input current becomes

$$\varphi_N \in [0, \frac{\pi}{6}]:$$
$$i_{N,R,\mathrm{avg},r} = \frac{2}{\sqrt{3}} M P_{O,r} \frac{\cos(\varphi_N) - 2M^{-1}\cos(\varphi_N)\cos(\varphi_N + \frac{\pi}{6}) + \frac{\sqrt{3}}{2} M^{-1}}{1 - M^{-1}\cos(\varphi_N)\cos(2\varphi_N + \frac{\pi}{6})}. \tag{42}$$

$$\varphi_N \in [\frac{\pi}{6}, \frac{\pi}{3}]:$$
$$i_{N,R,\mathrm{avg},r} = \frac{2}{\sqrt{3}} M P_{O,r} \frac{\cos(\varphi_N) + \frac{1}{2} M^{-1}\cos(2\varphi_N + \frac{\pi}{6})}{1 + M^{-1}\cos(\varphi_N - \frac{\pi}{3})\cos(2\varphi_N + \frac{\pi}{6})} \tag{43}$$

$$\varphi_N \in [\frac{\pi}{3}, \frac{\pi}{2}]:$$
$$i_{N,R,\mathrm{avg},r} = \frac{2}{\sqrt{3}} M P_{O,r} \frac{\cos(\varphi_N)\left(1 - M^{-1}\sin(\varphi_N)\right)}{1 - M^{-1}\cos(\varphi_N - \frac{\pi}{3})\sin(2\varphi_N)}. \tag{44}$$

For R_N we receive directly with (10) and (14)

$$R_N = \frac{3}{4} \frac{L_U}{T_P} M^{-2} P_{O,r}^{-1}. \tag{45}$$

$$I_{D,\mathrm{avg},r} = \frac{1}{2}\delta_P \left[\frac{3}{\pi}\left(\frac{M}{\sqrt{M^2-3}}(\tan^{-1}\frac{\sqrt{3}}{\sqrt{M^2-3}} + \tan^{-1}\frac{\frac{\sqrt{3}-1}{\sqrt{3}+1}M - \sqrt{3}}{\sqrt{M^2-3}}) + \frac{1}{2\sqrt{3}}\log(1 - \frac{\sqrt{3}}{2}M^{-1}) + \frac{\sqrt{3}}{4}M^{-2} + (1 - \frac{\sqrt{3}}{2})M^{-1}\right) + \frac{3}{8}M^{-2} - \frac{1}{4}\right]. \tag{36}$$

D. Fourier Analysis

According to the chosen position of the starting point $\varphi_N = 0$ of the phase angles within the fundamental and to the assumptions regarding symmetry (cf. Section III-A) there follow the Fourier coefficients of the mains current via

$$I_{N,(k),r} = \frac{4}{\pi} \int_0^{\frac{\pi}{2}} i_{N,r}(\varphi_N) \cos(k\varphi_N)\, d\varphi_N \qquad (46)$$
$$k = 1, 5, 7, 11, 13 \ldots .$$

For the amplitudes of the mains current harmonics we have

$$\hat{I}_{N,(k),r} = |I_{N,(k),r}| . \qquad (47)$$

The related fundamental of the mains current can be given directly by rating of the power balance equation (13) via

$$\hat{I}_{N,(1),r} = \frac{2}{\sqrt{3}} M P_{O,r}. \qquad (48)$$

E. Mains Filter

For the sake of brevity only a few important points for dimensioning of the mains filter (shown in Fig. 1 as simple single-stage type L_N, C_N) are given.

In general, dimensioning of L_N, C_N has to be performed such that the high frequency harmonics of $i_{U,(RST)}$ are suppressed and that an increase of the low frequency harmonics is avoided. Therefore, the low frequency harmonics of $i_{U,(RST)}$ basically are not influenced by the mains filter. They occur directly as mains current harmonics. Furthermore, the danger of excitation of the filter by ripple-control signals ($f <$ 1.4 kHz) has to be observed. The filter resonance frequency therefore has to be selected above 50 f_N. According to VDE 0871, the required damping at switching frequency has to be $>$ 80 dB for systems with output powers in the kW region. Due to this the filter has to be designed as a higher order type (e.g., 3 LC-stages) and a switching frequency $f_P > 500\ f_N$ is required. One has to keep in mind, however, that for a number of stages $>$ 3 further stages contribute only to a relatively small degree to the overall damping. More than one stage is also to be favored regarding the decreasing sensitivity of the filter characteristic with respect to the inner mains impedance. As, e.g., described in [16] and [17], for high dynamics of the voltage control loop one also has to include the input filter transfer function into the controller design.

Dimensioning of the filter with optimal damping and minimum weight and size in general is a very important aspect for the practical applicability of the system. This also is especially true because (as already evident by the high required damping) inclusion of volume and weight of the filter cuts the power density of the rectifier into about one half as compared to the case without filter. Therefore, also the filter cost will have a substantial influence on the overall system cost.

A reduction of the filtering effort can be achieved only by increasing f_P. Connected herewith, the extension of three-phase single-switch discontinuous-mode boost rectifiers to quasiresonant operation (as discussed in [9] and [10]) seems to be of special importance. An alternative to increasing f_P is given by paralleling of several systems which are pulsed with shifted phases. This method becomes economically interesting only for higher output power, however.

F. Comparison of the Control Methods

As the comparisons given in Fig. 6 makes clear, all control methods show a quality of the mains current being significantly dependent on M.

For $M > 5$ we have approximately purely sinusoidal current shape (or a shape proportional to the mains voltage, respectively). Due to U_O being relatively high compared to $\sqrt{3}\hat{U}_N$ the demagnetization of L_U will need only a minor part of the pulse period. The current rise being proportional to $u_{N,(RST)}$ within $t_\mu \in [0, t_{\mu,1}]$ therefore leads to local mean values $i_{U,(RST),\text{avg}}$ being also largely proportional to $u_{N,(RST)}$. This means also an approximate voltage-proportional shape of the mains currents $i_{N,(RST)}$. Generally, one has to strive for U_O as high as possible therefore.

Due to U_O = 660 V ... 820 V being present for an operation of the system in the European mains especially $M <$ 1.5 is of interest for a practical realization. For constant f_P and high dynamics of the control of u_O (control method III, cf. Fig. 6(c)) we obtain a reduction of the 5th harmonic of $i_{N,(RST)}$ in the region $M < 2.0$ as compared to the operation with constant $t_{\mu,1}$ (control method I, cf. Fig. 6(a)). However, this is connected with an increase of the 7th harmonic. When the system operates at the border of the discontinuous mode (control method II) there occurs a modulation of the duty cycle of T which is comparable to that given for constant $p_{O,\text{avg}}$ (cf. Fig. 7(b) and (c)). This results in an approximately similar shape of the dependency of the 5th and 7th harmonic on M (cf. Fig. 6(b) and (c)).

For $M < 1.25$ especially for control method I high amplitudes of the low frequency harmonics of $i_{N,(RST)}$ occur. There, the current shape within a pulse period and the local current mean value are mainly determined by the demagnetization phase. Due to the only low difference between peak value of the line-to-line voltages and U_O the relative duration of the second part $t_\mu \in [t_{\mu,2}, t_{\mu,3}]$ of the demagnetization interval is substantially increased as compared to higher U_O. This results in a wide gap for that phase current which shows the smallest absolute value in $t_{\mu,1}$. This gap finally causes the distortion of $i_{N,(RST)}$. Furthermore, in this region of operation an extremely low utilization factor of T has to be observed. The converter application therefore should be limited to $U_O >$ 3.0 $U_{N,\text{rms}}$ independent of the selected control method.

VI. Digital Simulation

The comparison of the results of the theoretical analysis performed in the previous section with a digital simulation (cf. Fig. 7) shows that the deviations are less than 1% for $f_P \geq 500\ f_N$. According to the assumtions of the analytical calculation ideal system behavior is also assumed for the digital simulation. Relative quantities like the mains current harmonics (rated to the fundamental) are influenced only in a very slight manner by these neglections. Therefore, the results of the analytical calculation allow a very accurate judgement of the mains behavior of the system.

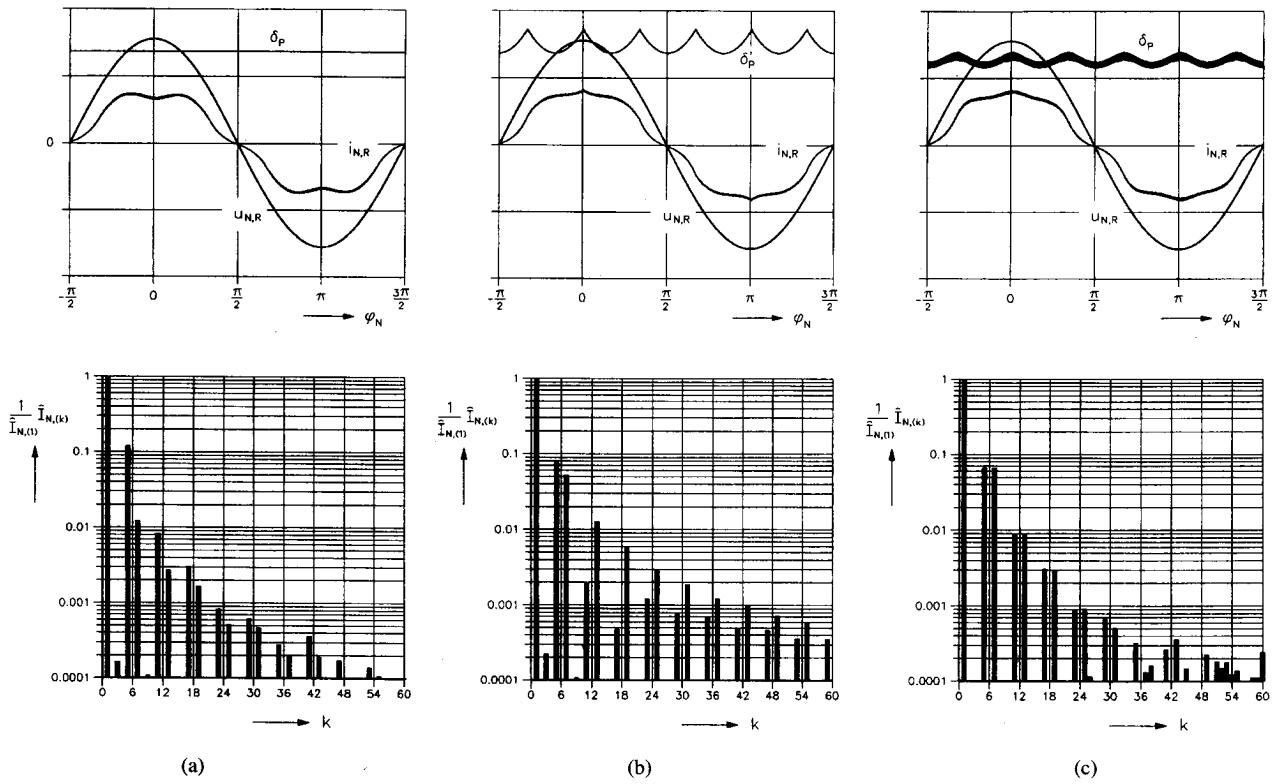

Fig. 7. Comparison of different control concepts by digital simulation of the system; ideal system components are assumed; representation of the mains phase voltage $u_{N,R}$ (200 V/div), of the related mains phase current $i_{N,R}$ (20 A/div) and of the relative turn-on time δ_P of T (for control method I and III) and of quantity δ'_P corresponding to the local switching frequency for control method II (cf. (21)), 0.5/div. Furthermore, representation of the amplitude spectrum of the mains current (related to the amplitude of the mains current fundamental $\hat{I}_{N,(1)}$). Parameters: $U_{N,\mathrm{rms}} = 220$ V, $U_O = 820$ V ($M = 1.52$), $f_N = 50$ Hz, $f_P = 45$ kHz, $L_U = 75\ \mu$H, $L_N = 250\ \mu$H, $C_N = 2.5\ \mu$F; (a) control method I: pulse frequency f_P and turn-on time of the power transistor $t_{\mu,1} = 7.6\mu$s constant over the fundamental period, $C = 4$ mF, $P_O = 6.875$ kW; (b) control method II: operation at the border of the discontinuous mode for constant turn-on time $t_{\mu,1} = 7.6\ \mu$s, $C = 4$ mF, $P_O = 7.5$ kW; (c) control method III: highly dynamical control of the output voltage for constant pulse frequency f_P, P-controller: $R(s) = k_P$, zero-crossing frequency of the voltage control loop: $f_O = 1.025$ kHz, $C = 1.0$ mF, $P_O = 7.5$ kW.

Besides the shape of mains voltage $u_{N,R}$ and mains current $i_{N,R}$ Fig. 7 also represents the relative turn-on time δ_P (for control methods I and III; cf. Fig. 7(a) and (c)) and the ratio $\delta'_P = t_{\mu,1}/t_{\mu,3}$ which characterizes the time shape of the local pulse frequency given for control method II (cf. Fig. 7(b)).

Because the current gap $t_\mu \in [t_{\mu,3}, T_P]$ is avoided if the system is operated at the border to continuous mode, for equal turn-on time $t_{\mu,1}$ control method II leads to an increased output power P_O as compared to constant f_P (control method I). In general, a relatively small additional effort regarding the converter control circuit results in a better utilization of the components of the power circuit. Nevertheless it has to be kept in mind that this operating mode leads to very high switching frequencies in the region of small output power. Therefore, a pulse frequency limitation has to be provided especially for systems with high rated power.

Fig. 7(c) shows the relationships for highly dynamic output voltage control. Besides the control error the controller $R(s)$ also amplifies the voltage ripple of the output capacitor C. This leads for a given zero-crossing frequency of the open loop gain to a relatively wide high-frequency variation of the turn-on time which is approximately independent of the capacitance value of C. For a practical realization a proper measurement filter has to be used, e.g., a measuring system which averages u_O over a pulse period.

Regarding the mains current spectrum the consistency between the digital simulation (cf. Fig. 7) and the analytical calculation (cf. Fig. 6) is determined essentially by the ratio of the pulse frequency f_P and the mains frequency f_N, by the dimensioning of the mains filter and by the voltage transformation ratio M.

According to Fig. 6 there occur high amplitudes of the low-frequency harmonics of the rectifier input current and/or of the mains current for low values of the voltage transformation ratio for all control methods. Therefore, in connection with the output impedance of the mains filter there results a (minor) low-frequency distortion of the filter output voltage. This deviation of the system input voltage (mains filter output voltage) from a sinusoidal shape as not considered in the analytical calculation leads to an influence of the mains current spectrum due to the current formation being linked directly to the input voltage. There, due to the system nonlinearity each voltage harmonic influences the amplitudes of all input current harmonics. E.g., the amplitude of the 7^{th} harmonic of the rectifier input current is dependent (to a low extent) also on the 5^{th} harmonic of the mains filter output voltage.

Therefore, the mains current harmonics as calculated by digital simulation (cf. Fig. 7) in connection with the investigation of the control methods deviate from the values as being calculated analytically for purely sinusoidal mains filter

output voltage (or, by neglecting the mains filter). E.g., there follows for control method I for the dimensioning of the system assumed in connection with Fig. 7 a relative amplitude of the 7th harmonic $\hat{I}_{N,(7)} = 0.012$ (cf. Fig. 7(a)); for purely sinusoidal shape of the filter output voltage we have $\hat{I}_{N,(7)} = 0.009$ according to Fig. 6(a). However, a noticeable deviation as compared to the analytical calculation (cf. Fig. 6) remains limited to harmonics with relative low amplitudes ≤1%. Such the amplitude of the 5th rectifier input current harmonic (being more dominant than the 7th) is only marginally influenced; for digital simulation we receive $\hat{I}_{N,(5)} = 0.118$ (cf. Fig. 7(a)), according to Fig. 6(a) we have $\hat{I}_{N,(5)} = 0.120$. The time shape of the mains current is only marginally influenced, therefore.

Remark: In connection with the previous discussion we want to point out that the assumption of an ideal sinusoidal and impressed filter output voltage represents a basic assumption for the analytically closed calculation of the mains current shape. This approximation of the real conditions can be justified because it is not the aim of the analytical calculation to describe the system behavior in dependency on essentially dimensioning-dependent parameters. The aim is in reality to obtain a comparison and evaluation of different control methods based (for the sake of clearness) on largely idealized conditions. For practical system application also the generally substantially higher harmonic content of the mains voltage (caused by single-phase rectifier circuits of mass production apparatus) is added to the filter output voltage distortion as caused by low frequency rectifier input current harmonics (in the case at hand we have $\hat{U}_{N,(5)} = 0.002$). The former leads to a further change of the amplitudes of the low-frequency current harmonics as compared to the values given in Fig. 6. (In the European low-voltage mains we have to consider typically voltage harmonics of $\hat{U}_{N,(5)} = 0.045$ [18].) A direct numerical comparison of the harmonics of the mains current shape measured on a test circuit being operated at the mains (cf. Fig. 8) and of the results of the analytical calculation is not appropriate, therefore.

VII. Experimental Results

As can be seen clearly from comparing Fig. 6 and Fig. 8, the theoretical considerations are consistent with the measurements on a laboratory model. For the sake of brevity, the representation of the measurements is limited to the converter operation with constant $t_{\mu,1}$ and constant f_P (control method I).

For minimizing the system cost one has to investigate the possibility to realize the three-phase diode bridge as rectifier module. Fig. 8 shows the situation for using such a module and for using discrete diodes with low reverse recovery time arranged as a three-phase bridge.

Due to the high reverse recovery time we experience a distortion of the diode bridge input currents, e.g., of $i_{U,R}$ (cf. Fig. 8(a)) if a rectifier module is applied. For high-speed diodes (cf. Fig. 8(b)) we have approximately ideal conditions. $i_{N,R}$ shows almost identical shape in both cases. The distortion of $i_{U,R}$ is limited to intervals of $\frac{\pi}{3}$ located symmetrical to the zero crossings of $i_{N,R}$. This can be explained by the fact that

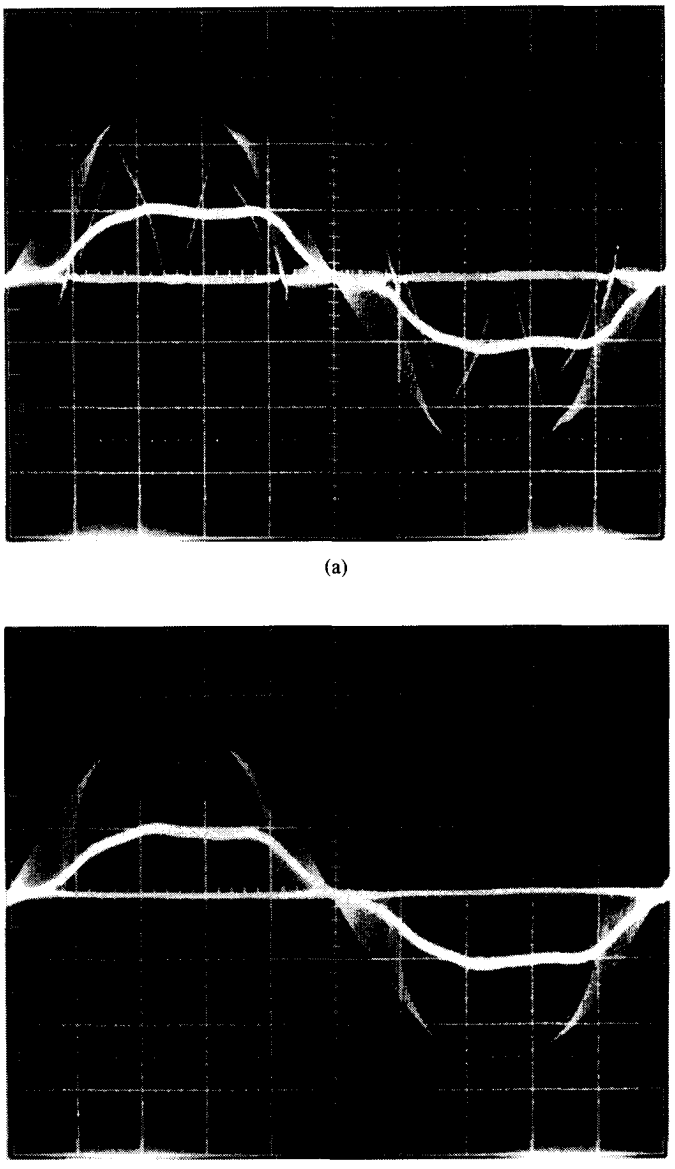

(a)

(b)

Fig. 8. Measurements on a 2.5 kW laboratory model of a three-phase single-switch discontinuous-mode boost rectifier; time behavior of the input current $i_{U,R}$ of the three-phase diode bridge and of the related mains phase current $i_{N,R}$ for control method I (constant $t_{\mu,1}$ and constant f_P); 10 A/div; parameters: $M = 1.5$, $U_{N,\mathrm{rms}} = 115$ V, $f_N = 50$ Hz, $f_P = 10.05$ kHz, $L_U = 75$ μH, single stage filter: $L_N = 1.2$ mH, $C_N = 22$ μF, $P_O = 2.5$ kW. realization of the diode bridge: (a) by using a three-phase rectifier module; (b) application of discrete diodes with low reverse recovery time arranged as three-phase bridge.

in this region a higher rate of decay of the current $i_{U,R}$ is encountered than in the rest of the mains period. In general, a higher rate of decay at the zero crossings of the input currents $i_{U,(RST)}$ is given for that phase which shows the smallest absolute current value at $t_{\mu,1}$. As shown in Section IV for $\varphi_N \in [0, \frac{\pi}{6}]$, only the projection of $\underline{u}_N - \underline{u}_{U,[100]}$ is effective after the end of the first phase of demagnetization in $t_{\mu,2}$ (cf. Fig. 5). Therefore, the zero crossings of $i_{U,R}$ and $i_{U,T}$ in $t_{\mu,3}$ show a smaller rate of decay than the zero crossing of $i_{U,S}$ in $t_{\mu,2}$. For higher switching frequency the current distortion can be experienced to a higher degree also in the other regions of φ_N. Therefore, the diode bridge has to be realized with

discrete semiconductors also because the diode losses would rise significantly.

VIII. Conclusions

As this paper shows, the effect on the mains of a three-phase single-switch discontinuous-mode boost rectifier system is essentially determined by the voltage transformation ratio and by the dynamics of the output voltage control. One has to point out that the results of the converter analysis given in this paper can be applied directly to the assessment of the mains behavior of a three-phase single-switch Ćuk rectifier [9], [11] and of further converters with equal structure of the input section [9].

In connection with the limitation of the harmonics stress on public mains (as enforced by regulations and standards) three-phase single-switch pulse rectifiers will gain increased importance in the future because of the simple structure of the power and control circuit. For industrial application of the converter especially the optimal dimensioning of the mains filter will be of importance. This is also true for the minimization of the increase of the input current distortion occurring for mains unsymmetries. Related investigations are the topic of further research at present.

Acknowledgment

The authors are very much indebted to the Austrian Fonds zur Förderung der Wissenschaftlichen Forschung which supports the work of the Power Electronics Section at their university.

References

[1] A. R. Prasad, P. D. Ziogas, and S. Manias, "An active power factor correction technique for three-phase diode rectifiers," *IEEE Trans. Power Electron.*, vol. 6, no. 1, pp. 83–92, 1991.

[2] N. Mohan, T. M. Undeland, and W. P. Robbins, *Power Electronics: Converters, Applications, and Design.* New York: Wiley, 1989.

[3] J. W. Kolar, H. Ertl, and F. C. Zach, "A comprehensive design approach for a three-phase high-frequency single-switch discontinuous-mode boost power factor corrector based on analytically derived normalized converter component ratings," *IEEE Trans Ind. Applicat.*, vol. 31, no. 3, pp. 569–582, 1995.

[4] K. H. Liu and Y. L. Lin, "Current waveform distortion in power factor correction circuits employing discontinuous-mode boost converters," in *Rec. 20th IEEE PESC*, Milwaukee, vol. II, pp. 825–829, June 26–29, 1989.

[5] J. W. Kolar, H. Ertl, and F. C. Zach, "Calculation of the passive and active component stress of three-phase PWM converter systems with high pulse rate," in *Proc. 3rd Europ. Conf. Power Electronics and Applications*, Aachen, vol. 3, Oct. 9–12, 1989, pp. 1303–1311.

[6] R. Erickson, M. Madigan, and S. Singer, "Design of a simple high-power-factor rectifier based on the Flyback converter," in *Rec. 5th IEEE APEC*, Los Angeles, pp. 792–801, Mar. 11–16, 1990.

[7] K. R. Jardan, S. B. Dewan, and G. R. Slemon, "General analysis of three-phase inverters," *IEEE Trans. Ind. General Applicat.*, vol. IGA-5, no. 6, pp. 672–679, 1969.

[8] S. Singer, and R. W. Erickson, "Canonical modeling of power processing circuits based on the POPI Concept," *IEEE Trans. Power Electron.*, vol. 7, no. 1, pp. 37–43, 1992.

[9] E. Ismail, and R. W. Erickson, "A single transistor three-phase resonant switch for high-quality rectification," in *Rec. 23rd IEEE PESC*, Madrid, vol. II, June 29–July 3, pp. 1341–1351.

[10] S. Gataríc, D. Boroyevich, and F. C. Lee, "Soft-switched single-switch three-phase rectifier with power factor correction," in *Proc. 9th IEEE APEC*, Orlando, vol. 2, Feb. 13–17, 1994, pp. 738–744.

[11] L. Malesani, L. Rossetto, G. Spiazzi, P. Tenti, I. Toigo, and F. Dal Lago, "Single-switch three-phase AC-DC converter with high power factor and wide regulation capability," in *Proc. 14th IEEE INTELEC*, Washington, D.C., Oct. 4–8, 1992, pp. 279–285.

[12] F. Lin and D. Y. Chen, "Reduction of power supply EMI emission by switching frequency modulation," in *Proc. 10th Annu. VPEC Power Electron. Seminar*, Blacksburg, VA, Sept. 20–22, 1992, pp. 129–136.

[13] I. Takahashi and Y. Itoh, "Electrolytic capacitor-less PWM inverter," in *Proc. Int. Power Electron. Conf.*, Tokyo, vol. 1, Apr. 2–6, 1990, pp. 131–138.

[14] H. Akagi, Y. Kanazawa, and A. Nabae, "Generalized theory of the instantaneous reactive power in three-phase circuits," in *Proc. Int. Power Electron. Conf.*, Tokyo, vol. 2, Mar. 27–31, 1983, pp. 1375–1386.

[15] W. Schott and M. Herfurth, "Switched mode power supply with power factor correction," in *Proc. 6th Int. Conf. Power Electron. and Motion Control*, Budapest, vol. 2, Oct. 1–3, 1990, pp. 64–68.

[16] F. C. Lee and Y. Yu, "Input filter design for switching regulators," *IEEE Trans. Aerosp. Electron. Syst.*, vol. AES-15, no. 5, pp. 627–634, 1979.

[17] A. S. Kislovski, R. Redl, and N. O. Sokal, *Dynamic Analysis of Switching-Mode DC/DC Converters* New York: Van Nostrand Reinhold, 1991.

[18] R. Gretsch and W. Gunselmann, "Harmonic distortion of the mains voltage by switched-mode power supplies—Assessment of the future development and possible mitigation measures," in *Proc. 3rd Europ. Conf. Power Electron. and Applications*, Aachen, vol. 3, Oct. 9–12, 1989, pp. 1255–1260.

Johann W. Kolar (M'89) was born in Upper Austria on July 15, 1959. He is currently working toward the Ph.D. degree at the Technical University of Vienna in the area of analysis and control optimization of single-phase and three-phase PWM rectifier systems.

He is with the Power Electronics Section, Technical University of Vienna, Austria, and is involved as a consultant in several industrial research and development projects on ac line conditioning and on switched-mode power supplies. He also does research in the areas of inverter and converter development and of theoretical analysis of power electronic systems. He is the author of numerous technical and scientific papers and patents.

Mr. Kolar received the award of the Power Systems Engineering Society (ÖGE) of the Austrian Institute of Electrical Engineers (ÖVE) for his research on the minimization of the mains current distortion of three-phase ac-dc converter systems.

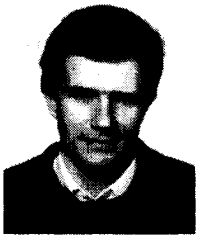

Hans Ertl (M'93) was born in Upper Austria on May 28, 1957. He received the Dipl.Ing. degree from the Technical University Vienna, Austria, in 1984, and the Ph.D. degree in 1991.

Since 1984, he has been a Scientific Assistant in the Power Electronics Section, Technical University Vienna. His current activities are in the area of PWM converter systems and switched mode power supplies. He is the author of various technical and scientific paper and patents.

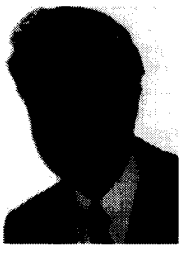

Franz C. Zach (M'82) was born in Vienna, Austria, on December 5, 1942. He received the Dipl.Ing. and Ph.D. degrees (cum laude) from University of Technology, Vienna, in 1965 and 1968, respectively.

From 1965 to 1969, he was a Scientific Assistant in Vienna. From 1969 to 1972, he was with NASA Goddard Space Flight Center, Greenbelt, MD. In 1972, he joined the Vienna University of Technology as an Associate Professor, where he has been heading the Power Electronics Section since 1974. He is the author of numerous technical and scientific papers and patents, and of two books on automatic control and power electronics. His current activities lie in power electronics and associated controls, especially as used for variable-speed ac and dc motor drives and power supplies. He is also involved in extensive industrial work in these areas.